

# Reconstruction of the Toroidal Flow Profile of a Field-Reversed Configuration Plasma<sup>\*)</sup>

Yasuyuki FUJIKAWA, Tomohiko ASAI, Midori GOUDA, Tsutomu TAKAHASHI,  
Loren C. STEINHAUER<sup>1)</sup> and Toshiki TAKAHASHI<sup>2)</sup>

*College of Science and Technology, Nihon University, 1-8-14 Kanda-Surugadai, Chiyoda, Tokyo 101-8308, Japan*

<sup>1)</sup>*Department of Aeronautics and Astronautics, University of Washington*

<sup>2)</sup>*Department of Electronic Engineering, Gunma University, 1-5-1 Tenjin-cho, Kiryu, Gunma 376-8515, Japan*

(Received 10 December 2011 / Accepted 13 July 2012)

Strong toroidal flow is spontaneously generated in a field-reversed configuration (FRC) plasma. It is continuously accelerated during and after the formation phase. The centrifugal force resulting from the toroidal flow causes deformation of the toroidal cross section, with toroidal mode number  $n = 2$ . The radial profile of this self-generated toroidal flow has previously been described as rigid rotor (RR) in form, i.e., showing uniform angular velocity. However, the toroidal flow profile observed in these experiments indicates the existence of flow shear. In this work, reconstruction of such a profile, utilizing a modified Abel inversion technique, has been performed, and the resulting detailed toroidal flow profile, including time evolution, has been investigated.

© 2012 The Japan Society of Plasma Science and Nuclear Fusion Research

Keywords: field-reversed configuration,  $n = 2$  mode rotational instability, toroidal flow, ion Doppler spectroscopy, Abel inversion, rigid rotor, two-point equilibrium

DOI: 10.1585/pfr.7.2402130

## 1. Introduction

A field-reversed configuration (FRC) plasma has a strong self-generated toroidal flow, which is continuously spun-up during and after the formation phase. This causes rotational deformation of the toroidal section, with toroidal mode number  $n = 2$ , and this instability eventually terminates the configuration lifetime. Several candidates for the physical mechanism of this toroidal spin-up have been proposed, such as selective ion loss [1], end-shortening [2], and flux-decay [3]. A rigid rotor (RR) model [4] has been recognized as an equilibrium rotation model for FRC which agrees with the results from experimentally generated FRC plasma. Recently, a two-point equilibrium (2-PE) model [5] has also been presented as a more accurate rotation profile model.

In previous experiments performed on the NUCTE (Nihon University Compact Torus Experiment)-III device, the toroidal flow profile  $\bar{v}_\theta$  and its time evolution have been observed using an ion Doppler spectroscopy (IDS) technique involving line integrated optical measurement for the line spectrum of impurity carbon [6]. However, preliminary observation has revealed a profile which does not agree with the RR model.

Therefore, in this work, radial profile of toroidal flow  $v_\theta(r)$  is reconstructed by modified Abel inversion technique from the line integrated shifted Gaussian emission profile. The flow profile of  $v_\theta(r)$  is also reconstructed according to

the flow profile of the RR model (uniform angular velocity profile), and is compared with the Abel inversion one to assess the credibility of the obtained radially non-uniform angular velocity profile.

Also fluctuations on the time evolution of toroidal flow are examined to evaluate effectiveness of global motion of FRC plasma onto the reconstruction and to discuss the cause of toroidal spin-up.

## 2. Experimental Device and Diagnostics

The FRC plasma was formed using a field-reversed theta-pinch (FRTP) method on the NUCTE-III device [7]. The schematic view of the NUCTE-III is shown in Fig. 1. This device has a transparent fused quartz discharge tube of 0.256 m in diameter and 2.0 m in length as the main discharge chamber. A 1.5 m long one-turn solenoidal theta-pinch coil surrounds the discharge tube. Each coil element has a 5.0 mm slit at intervals of 50 mm, enabling optical measurements through a collimator and optical fiber tube.

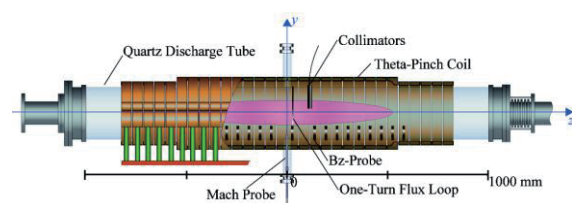


Fig. 1 Schematic diagram of the NUCTE-III with diagnostics.

author's e-mail: csya10028@g.nihon-u.ac.jp

<sup>\*)</sup> This article is based on the presentation at the 21st International Toki Conference (ITC21).

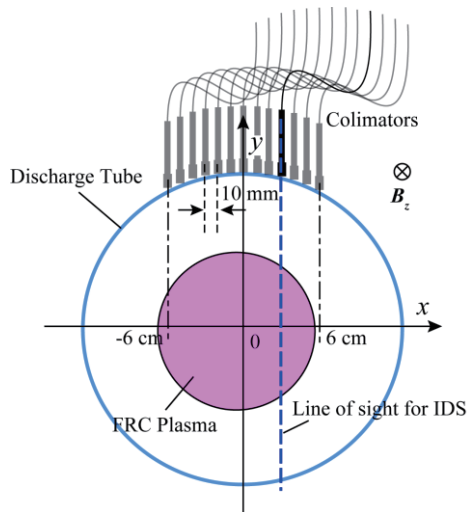


Fig. 2 Measurement positions of the IDS system on a toroidal cross section.

This theta-pinch coil consists of a 0.9 m-long center region with 0.17 m I.D., and two 0.25 m-long end mirror regions with 0.15 m I.D.

The FRC plasma formed by the NUCTE-III has a separatrix radius of 0.06 m, plasma length of 0.8 m, total temperature of 300 eV, and electron density of  $3 \times 10^{21} \text{ m}^{-3}$ . A magnetic flux loop and magnetic probes are mounted on the discharge tube surface to measure magnetic flux using the excluded flux method. Electron density is measured by a single chord  $3.39 \mu\text{m}$  He-Ne laser interferometer. The wobble motion ( $n = 1$  oscillation mode) of the FRC is tracked by an array of 14 optical collimators arranged along the  $x$  and  $y$  axes at intervals of 1 cm. The measured wavelength band is selected by an interference band-pass optical filter with wavelength range of  $550 \pm 5 \text{ nm}$ . This bandwidth range has been confirmed in the NUCTE-III experiments as having no strong line spectra from impurity and deuterium ions and/or neutrals [8]. Therefore, the optical system can observe the  $x$  and  $y$  profile of Bremsstrahlung. The motion of the center position, created by the wobble motion is estimated using the obtained profiles.

The IDS system has been employed to measure the temperature and flow velocity of ions based on Doppler broadening and shifts in the line spectrum profile. In this series of experiments, IDS estimates the temperature and velocity of the impurity carbon (CV: 227.2 nm). The system consists of a collimator, a quartz optical fiber tube, a Czerny-Turner monochromator, and a 16 channel photomultiplier tube. The wavelength resolution is 0.04 nm per channel. The measurement position of the IDS on a toroidal cross section is shown in Fig. 2. The IDS scans over the range from  $x = -6$  to  $+6$  cm at intervals of 1 cm.

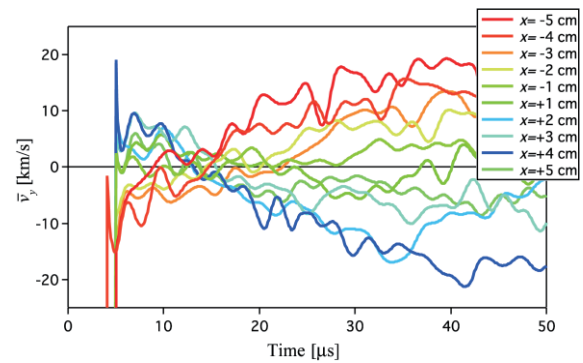


Fig. 3 Time evolution of the toroidal flow  $\bar{v}_y$  along the chords parallel to the  $y$  axis. Each curve has an oscillation with a cycle of  $3 \mu\text{s}$ .

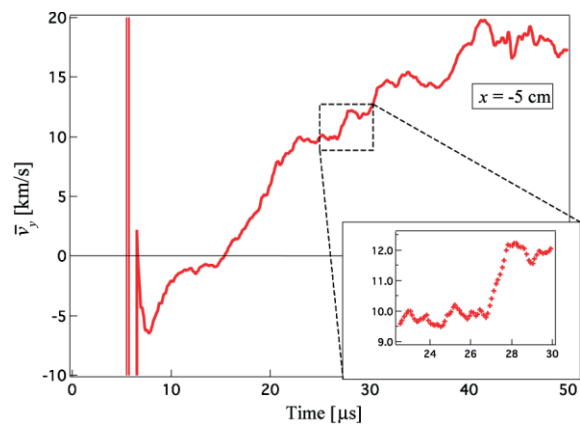


Fig. 4 Enlarged time evolution of the toroidal flow, showing oscillations with two different frequencies.

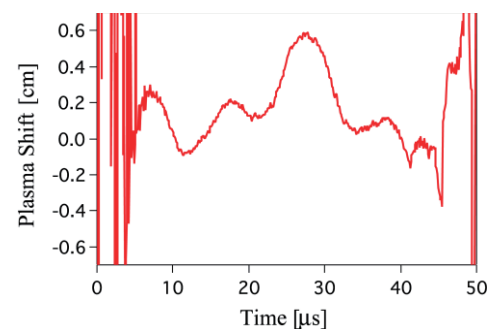


Fig. 5 The wobble ( $n = 1$ ) motion in the same FRC discharge as in Fig. 4.

### 3. Experimental Results

#### 3.1 Time evolution of toroidal flow velocity

Figure 3 shows the time evolution of the toroidal flow profile  $\bar{v}_y(x)$  evaluated from line-integrated line spectra, which are measured along the chords parallel to the  $y$  axis at the mid-plane ( $z = 0$ ). The origin of the  $x$  axis is set at the center of the discharge chamber. The wobble plasma motion ( $n = 1$ ) is not compensated for in these results. Each

curve is generated over multiple FRC discharges under the same experimental conditions.

We can see a toroidal flow in the paramagnetic direction just after the formation process, until around  $t = 12 \mu\text{s}$ . Then, at around  $t = 15 \mu\text{s}$ , the rotation direction is reversed into the diamagnetic direction. Then the flow accelerates until the end of the configuration lifetime. Eventually, at around  $25 \mu\text{s}$ , the toroidal flow velocity becomes comparable to the ion diamagnetic velocity.

The toroidal flow reveals major oscillations, with two different frequencies, as shown in Figs. 3 and 4. These oscillations appear even after noise reduction of the raw data using the fast Fourier transform (cut-off frequency of 400 kHz) (Fig. 3) and moving-average methods (cut-off frequency of 200 kHz) (Fig. 4). The higher oscillation shown in Fig. 3 (frequency: 250~400 kHz) is comparable to the “cycle of torque” possibly caused by an end-shortening event [9]. Figure 5 shows the time evolution of wobble plasma motion in the  $y$  direction, measured by the  $y$ -collimator array, for the same discharge as in Fig. 4. The oscillation of the lower frequency (180~200 kHz) shown in Fig. 4 is consistent with the frequency of wobble plasma motion.

### 3.2 Radial distribution of toroidal flow

More precise radial distribution of toroidal flow has been estimated through compensation for the wobble motion. In this process, the acquired data is averaged over a time window of  $6 \mu\text{s}$ . The displacement of plasma axis due to the wobble plasma motion along the  $x$  axis has been monitored by the optical fiber tube array. Then the measurement position of  $x$  is converted into the impact parameter  $x'$  to the plasma axis. The resulting time evolution of the toroidal flow is shown in Fig. 6. In the formation phase ( $8 \mu\text{s}$ ), the toroidal flow rotates in a paramagnetic direction with respect to the main compression field; and then, at around  $t = 12 \mu\text{s}$ , it flips into the diamagnetic direction. Then, until the onset time of rotational mode instability ( $t = 40 \mu\text{s}$ ), the diamagnetic rotation continuously accelerates, with the toroidal flow eventually attaining a speed comparable to the ion diamagnetic drift velocity, at  $t = 28 \mu\text{s}$ .

During this acceleration period, the toroidal flow velocity in the vicinity of separatrix ( $x \sim 6 \text{ cm}$ ) is less than that of the flow in the inner region. This indicates that the RR model is inapplicable to this experimentally observed plasma flow.

Figure 7 shows the flow profile directly calculated from the line-integrated data in comparison with the RR profile. As the figure indicates, the two profiles are not in agreement. To evaluate the accuracy of the reconstruction, an experimentally measured profile of the line spectra is compared with calculated profiles based on the RR model, as shown in Fig. 8. Here the shaded area shows the standard deviation on the experimentally observed profile due to the repeatability of plasma shots. Experimentally observed spectrum profile has significant difference from the

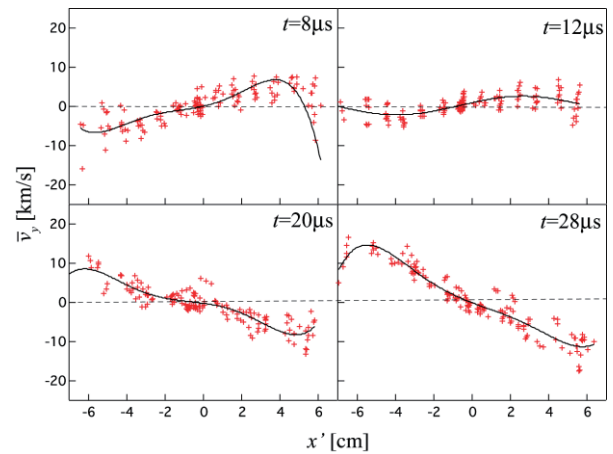


Fig. 6 Time evolution of the toroidal flow profile  $\bar{v}_y$  with respect to the  $x'$  axis at  $z = 0$ .

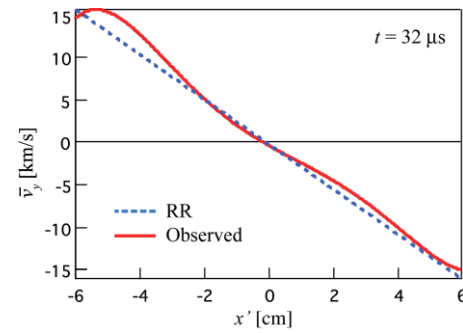


Fig. 7 Radial profile of RR (blue dashed line) and experimentally observed (red solid line) toroidal flow.

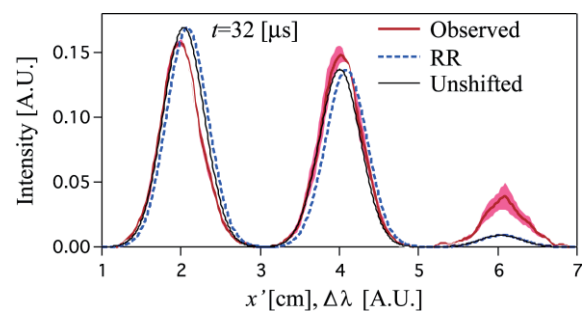


Fig. 8 Comparison between the line spectrum profiles with Doppler shift and broadening for  $x = 2, 4$  and  $6 \text{ cm}$ . The red line indicates the experimentally observed shifted spectrum; blue, the RR profile calculated for the experimental conditions; and black, the spectrum shape without Doppler shift. Red shading denotes the standard deviation.

one for RR profile. Therefore, the obtained line integrated profile seems to indicate the non-uniform angular velocity profile.

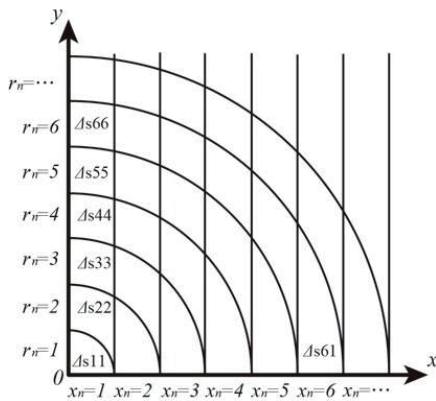


Fig. 9 Schematic of the dividing mesh structure for the Abel inversion.

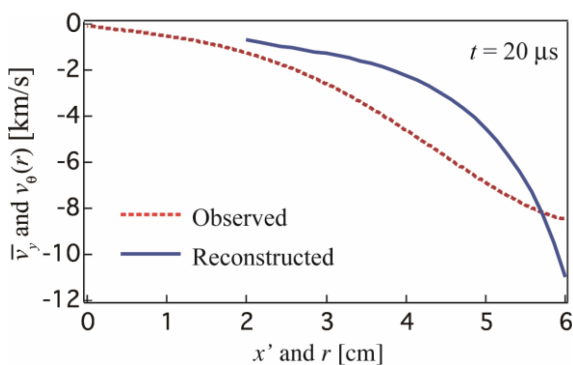


Fig. 10 Comparison between toroidal flow profiles calculated directly from line-integrated spectrum (Observed: red dashed line) and reconstructed by the Abel inversion (Reconstructed: blue solid line).

## 4. Reconstruction of the Spectrum Profile

A modified Abel inversion technique has been employed to reconstruct the line spectrum profile. The observed flow profile is based on the line integrated optical measurement. Therefore, the amount of Doppler shift and broadening have been attempted to be determined on the reconstructed spectrum. A schematic diagram of the dividing mesh structure for the Abel reconstruction is shown in Fig. 9.

The reconstruction assumes FRC axisymmetry. Each cell experiences a different amount of Doppler shift, and therefore the wavelength profile must be reconstructed with consideration of this spatial structure of the flow. Preliminarily, the Pearce method has been employed to solve the system equation. The reconstructed flow profile for the FRC plasma in an equilibrium phase is shown in Fig. 10. While the reconstructed flow profile has significant error in the vicinity of the geometrical axis, it shows larger shear just inside the separatrix ( $5 \text{ cm} < r < 6 \text{ cm}$ ).

## 5. Discussion

Oscillations with two different frequencies have been found in the time evolution of the toroidal flow, as shown in Figs. 3 and 4. The oscillation with the lower frequency is consistent with that of the wobble plasma motion. The higher frequency oscillation, on the other hand, is in close agreement with the ‘cycle of torque’ potentially caused by an end-shortening event.

Toroidal flow profiling using the IDS technique has revealed that the experimentally observed flow profile does not agree with the RR profile, as shown in Fig. 7, where a significant difference in flow profile is noticeable, especially in the inner region of the separatrix. Reconstruction of the radial structure of the shifted Gaussian spectrum has been attempted. However, this preliminary calculation still potentially has significant error in the vicinity of the geometrical axis. To increase the accuracy of the reconstruction, more precise monitoring of the plasma position and greater precision in the reconstruction calculation must be achieved.

## 6. Summary

Reconstruction of the toroidal flow profile of FRC plasma has been performed. The results indicate the following three facts. First, the toroidal flow has two different frequency components. The higher may be related to pulsed torque due to end-shortening. Another component corresponds to the wobble motion of the plasma column. Second, the spontaneous FRC toroidal flow begins in the paramagnetic direction and then accelerates in the diamagnetic direction. Third, the result of IDS measurement indicates the existence of radial flow shear. In addition, beyond the separatrix, Mach probe measurement [10] suggests that the angular velocity of the toroidal flow is non-uniform.

- [1] D.S. Harned and D.W. Hewett, Nucl. Fusion **24**, 201 (1984).
- [2] L.C. Steinhauer, Phys. Plasmas **15**, 012505 (2008).
- [3] T. Takahashi, H. Yumura, F.P. Iizima *et al.*, Plasma Fusion Res. **2**, 008 (2007).
- [4] R.L. Morse and J.P. Freidberg *et al.*, Phys. Fluids **13**, 0531 (1969).
- [5] L.C. Steinhauer and T.P. Intrator, Phys. Plasmas **16**, 072501 (2009).
- [6] T. Asai, Y. Matuzawa, N. Yamamoto *et al.*, In 17th International Toki Conference (ITC/ISHW2007) P1-015.
- [7] T. Asai, T. Takahashi, T. Kiguchi *et al.*, Phys. Plasmas **13**, 072508 (2006).
- [8] T. Takahashi, H. Gota, T. Fujino *et al.*, Rev. Sci. Instrum **75**, 5205 (2004).
- [9] L.C. Steinhauer, Phys. Fluids **24**, 328 (1981).
- [10] Y. Komoriya, Y. Hirayama, Y. Fujikawa *et al.*, in 19th international Toki Conference (ITC/ISHW2009) P2-033.